USGS
science for a changing world

Fluorescent Tracer Experiment on Holiday Beach near Mugu Canyon, Southern California

By Nicole Kinsman, Alaska Department of Natural Resources, and J. P. Xu, U.S. Geological Survey

Open-File Report 2012–1131

U.S. Department of the Interior
U.S. Geological Survey

Cover: Photograph of fluorescent tracer injection at the experimental Holiday Beach site, near Mugu Canyon in southern California (USGS photograph).

Back cover: Panoramic photograph of tracer delivery to Holiday Beach (USGS photograph).

Fluorescent Tracer Experiment on Holiday Beach near Mugu Canyon, Southern California

By Nicole Kinsman, Alaska Department of Natural Resources, and J. P. Xu, U.S. Geological Survey

Open-File Report 2012–1131

U.S. Department of the Interior
U.S. Geological Survey

U.S. Department of the Interior
KEN SALAZAR, Secretary

U.S. Geological Survey
Marcia K. McNutt, Director

U.S. Geological Survey, Reston, Virginia: 2012

Suggested citation:
Kinsman, N., and Xu, J.P., 2012, Fluorescent tracer experiment on Holiday Beach near Mugu Canyon: U.S. Geological Survey Open-File Report 2012-1131. (Available at *http://pubs.usgs.gov/of/2012/1131/*.)

Contents

Figures

Tables

Conversion Factors

Inch/Pound to SI

Multiply	By	To obtain
	Length	
inch (in.)	2.54	centimeter (cm)
inch (in.)	25.4	millimeter (mm)
foot (ft)	0.3048	meter (m)
mile (mi)	1.609	kilometer (km)
	Volume	
cubic foot (ft^3)	28.32	liter (L)
cubic foot (ft^3)	0.02832	cubic meter (m^3)

SI to Inch/Pound

Multiply	By	To obtain
	Length	
millimeter (mm)	0.03937	inch (in.)
centimeter (cm)	0.3937	inch (in.)
meter (m)	3.281	foot (ft)
meter (m)	1.094	yard (yd)
kilometer (km)	0.6214	mile (mi)
kilometer (km)	0.5400	mile, nautical (nmi)
	Area	
square centimeter (cm^2)	0.1550	square inch (ft^2)
square centimeter (cm^2)	0.001076	square foot (ft^2)
square meter (m^2)	0.0002471	acre
square meter (m^2)	10.76	square foot (ft^2)
	Volume	
cubic centimeter (cm^3)	0.06102	cubic inch (in^3)
cubic meter (m^3)	264.2	gallon (gal)
cubic meter (m^3)	35.31	cubic foot (ft^3)
cubic meter (m^3)	1.308	cubic yard (yd^3)
liter (L)	33.82	ounce, fluid (fl. oz)
liter (L)	2.113	pint (pt)
liter (L)	1.057	quart (qt)
liter (L)	0.2642	gallon (gal)
liter (L)	61.02	cubic inch (in^3)
	Speed	
centimeter per second (cm/s)	0.0328084	feet per second (ft/s)
centimeter per minute (cm/s)	0.0328084	feet per minute (ft/m)
	Density (Thickness)	
gram per cubic centimeter (g/cm^3)	62.4220	pound per cubic foot (lb/ft^3)

The Kumbein phi scale for grain size also is used within this report. To find a metric diameter (D) in mm using a phi (ϕ) value, use the equation below.

$$D = 2^{-\phi}$$

Fluorescent Tracer Experiment on Holiday Beach near Mugu Canyon, Southern California

By Nicole Kinsman, Alaska Department of Natural Resources, and J. P. Xu, U.S. Geological Survey

Abstract

After revisiting sand tracer techniques originally developed in the 1960s, a range of fluorescent coating formulations were tested in the laboratory. Explicit steps are presented for the preparation of the formulation evaluated to have superior attributes, a thermoplastic pigment/dye in a colloidal mixture with a vinyl chloride/vinyl acetate copolymer. In September 2010, 0.59 cubic meters of fluorescent tracer material was injected into the littoral zone about 4 kilometers upcoast of Mugu submarine canyon in California. The movement of tracer was monitored in three dimensions over the course of 4 days using manual and automated techniques. Detailed observations of the tracer's behavior in the coastal zone indicate that this tracer successfully mimicked the native beach sand and similar methods could be used to validate models of tracer movement in this type of environment. Recommendations including how to time successful tracer studies and how to scale the field of view of automated camera systems are presented along with the advantages and disadvantages of the described tracer methodology.

Introduction

Littoral sands are in high demand for coastal management purposes such as beach replenishment. With projections of rising sea levels in the upcoming decades, this demand for sand resources likely will increase. On the U.S. West Coast much of this littoral sand is thought to be lost into various submarine canyons that incise across a narrow continental shelf and intercept littoral transport (for example, Monterey, Hueneme, and Mugu Canyons in California). Trapping this part of the littoral sand budget before it is lost into canyons has been proposed by many coastal managers (for example, Moffatt and Nichol, 2008). However, the proportion of sand in a littoral system that is lost into a canyon and the amount that is bypassed to the downcoast portion of the beach remains unquantified. Knowledge of this partition is a key prerequisite for the human interception of littoral sand in order to avoid potential negative consequences to downcoast beach stability and unnecessary costs.

Mugu submarine canyon in southern California has been commonly cited as a near-complete sink at the downcoast boundary of the Santa Barbara Littoral Cell (Everts and Eldon, 2005; Patsch and Griggs, 2006). As part of a larger project to examine sand movement in the littoral zone near the head of Mugu submarine canyon, a fluorescent sand tracer study was conducted on an intertidal beach west (upcoast) of the canyon head (fig. 1). The results of this tracer experiment have been used to seed a numerical model that can be used to examine sand movement in the littoral zone near the head of Mugu canyon and to determine if sand is able to bypass the canyon head and in what quantities under predominant wave conditions (Xu and others, 2011).

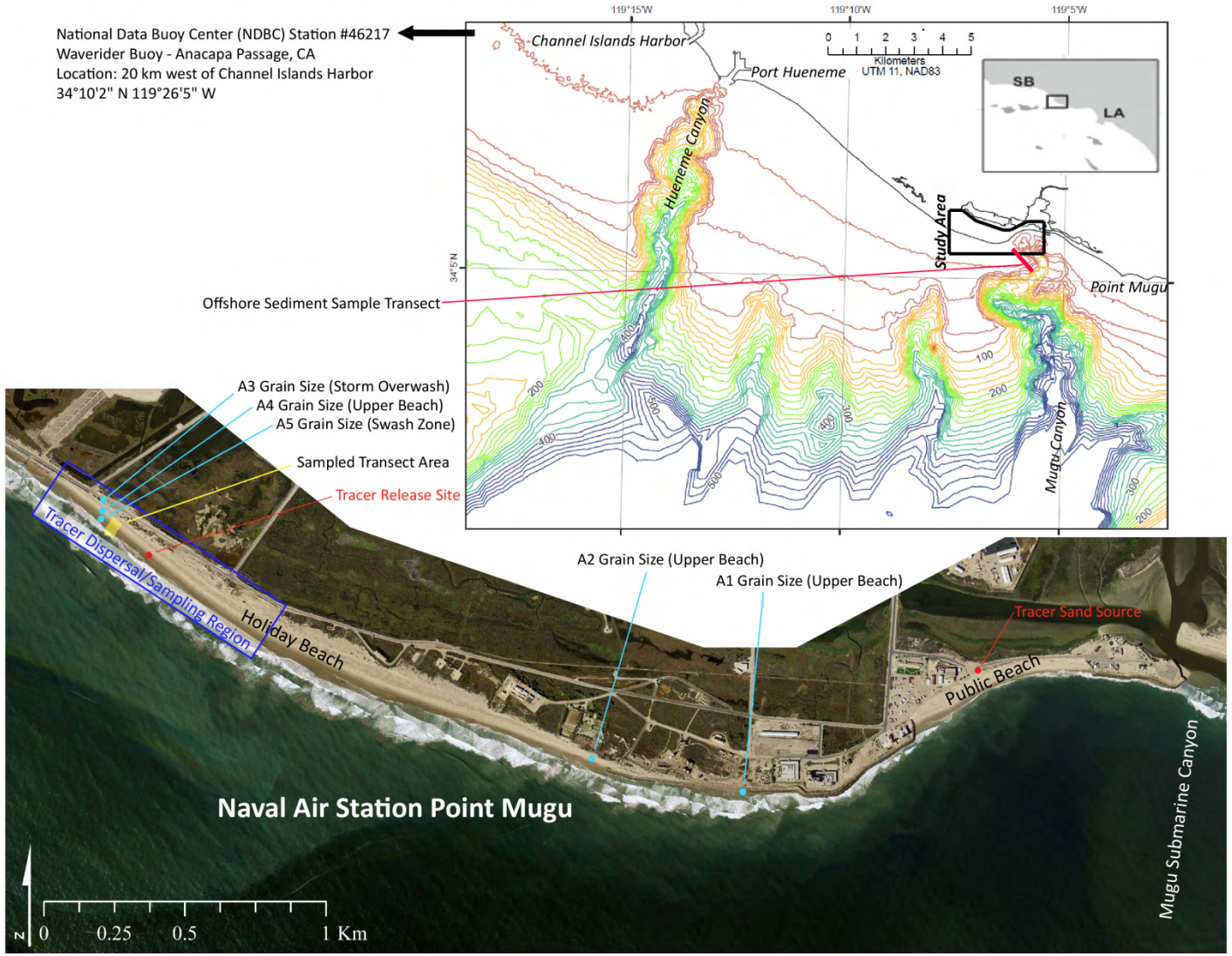

Figure 1. Map showing location of 2010 tracer experiment site on Holiday Beach near Mugu Canyon, southern California (USGS orthorecified aerial photograph, October 1, 2004). The Tracer Dispersal/Sampling Region (blue rectangle) encompasses the area in which tracer grain counts were conducted.

The first part of this report documents the processes and procedures of making fluorescent sand tracers from native beach sands. As noted by Ciavola (2004), there are few publications that detail sand marking techniques and the most well-known manual for creating coated tracers dates back to a half-century ago (Ingle, 1966). Therefore, the steps involved in tracer production are presented in detail for ease of use by future researchers. The second half of this report describes the deployment and ensuing surveys of the fluorescent sand tracers in the intertidal environment including recommendations for improved field studies of this type.

Making Fluorescent Tracers

Tracers have been incorporated into littoral zone studies as far back as 1902 for their ability to aid in qualitative and quantitative assessments of how sediments behave in coastal environments. The types of tracers used by these studies have taken a variety of forms (for a complete history, see Ciavola, 2004; Black and others, 2007). Non-natural sand-sized tracers fall into three general categories: radioactive tagging, artificial grains, and colored sediments. Once an efficient method of obtaining high tracer recovery rates, radioactive marking (for example, Heathershaw and Carr, 1977) is no longer an acceptable practice due to negative environmental impacts. Artificial tracer grains that mimic native sand are prohibitively expensive for use in experiments that require large volumes of tracer. The coloring of native sediments is the oldest type of artificial tracer and remains the most widely accepted and least expensive option available to littoral studies today (2012). In the 1960s, the use of fluorescent pigments that glow under ultraviolet (UV) light made recovery and tracer counts easier, and the use of these pigments for tracer production became common practice (Zenkovich, 1965; Teleki, 1966).

Sand Source

To ensure that tracer grains accurately mimic the behavior of native sediments, sand for tracer production should be sourced locally from the study area. Holiday Beach was selected as the site for this experiment primarily because of its position relative to Mugu submarine canyon (fig. 1). Additionally, the beach is located within the boundaries of the Point Mugu Naval Air Station. The advantage of conducting this type of experiment on the premises of a security-controlled U.S. military base is that it minimizes the likelihood of the tracer being disturbed by anthropogenic activities.

Sand for tracer production was collected in April 2010, approximately 5 months prior to the tracer release. At this time, access to the release site was limited, so 1.3 m^3 of sand was bagged for production from a pile of sand located adjacent to the Public Beach parking area (fig.1); collected sediment was composed of road-overwash sand from a February 2010 storm event. Grain size analyses (obtained by sieving) of sand samples taken from the release site exhibited a uni-modal distribution of medium sand that is moderately well sorted with a mean grain size (D_{50}) of 1.7–1.4 phi (310–390 μm in diameter). Grain size analyses of samples taken from the source pile exhibited strong agreement in grain size distribution with the source pile sand at the time of sand collection (black and gray bars, fig. 2). However, grain size analyses of samples collected from the release site at the time of tracer injection in September 2010 indicate a shift toward fines in the grain size distribution (blue bars, fig. 2). This variance in the grain size distributions over time resulted in the tracer material having a different distribution than the native sand at the experiment site; variance could be reduced by minimizing the amount of time between sand collection and release, to minimize the effects of seasonal variation in the wave environment.

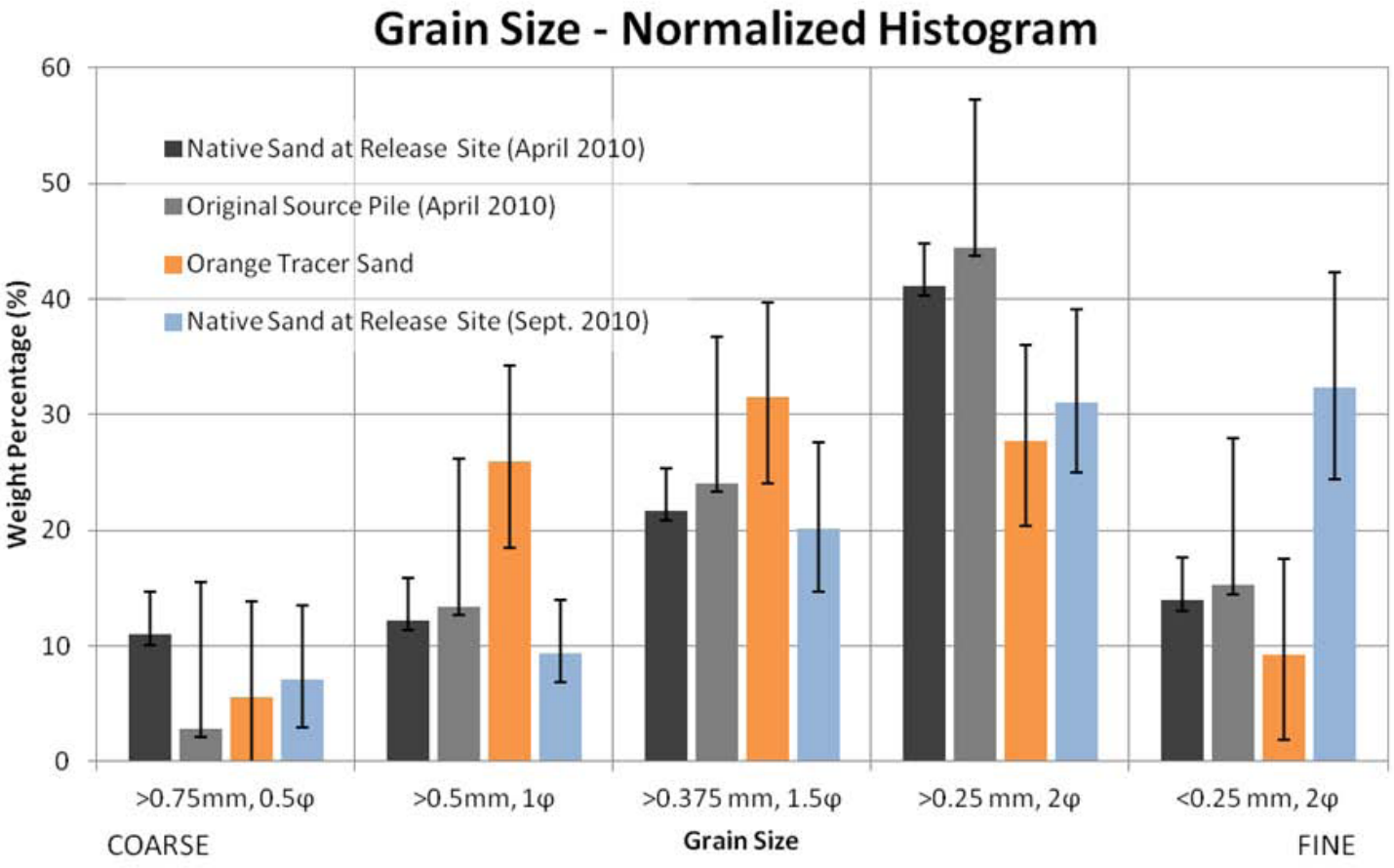

Figure 2. Histograms showing grain size distributions of sediment samples from around the experiment site.

Formulations

Native beach sand can be fluorescently tagged by one of two methods: (1) by staining the grains with a fluorescent dye/ink, or (2) by covering the grains in a thin fluorescent coating (for specific examples of each see Ingle, 1966). Ideally, tracer stains and coatings should be insoluble in seawater, resistant to abrasion in the surf zone, resistant to fading or losing UV properties over the study duration, nontoxic to sea-life, affordable, and thin enough to not substantially alter the hydrodynamic properties of the original sand grains. Stained tracers are reported to have longer lifespans in the surf zone than coated tracers (Chapman and Smith, 1977), but they are not well-suited for use on beaches with a dark mineral component. Because of the typical mineral composition of California beaches, grain-coating methods were investigated to create the fluorescent sand tracers for this experiment.

The creation of coated tracers involves the attachment of fluorescent pigments to native sand grains with the use of a binding agent. Few tracer studies adequately describe the types of fluorescent substances and binding agents that can be used for self-production. Multiple studies refer to the set of methods presented by Yasso (1966) (for example, Schwartz, 1966; Ciavola and others, 1997; Ferreira and others, 2002). Tracer production methods described by other studies involve paint/varnish binders (for example, Ciavola and others 1997a; Silva and others, 2007), plastic binders (for example, Jolliffe, 1963) or resin binders (for example, Teleki, 1966; Boon 1970). Each one of these three categories of binders was tested in a laboratory phase of this tracer experiment (table 1).

Table 1. Three different categories of tracer formulations that were tested in the laboratory.

Formulation	Fluorescent Pigment	Binding Agent	Category	Formulation Source
K1	DayGlo® A/AX Pigments in Acrylic Laquer	A.R. Monteith Acrylic Laquer 202 Line (204-04, Red Orange)	Paint/Varnish	Formulation #2, Yasso (1966)
K2	DayGlo® A-14N Pigment (Fire Orange)	Cytec Cymel U-227-8 Butylated Urea-formaldehyde Resin	Resin	Modified Formulation #3, Yasso (1966) and Procedure 5 in Ingle (1966) after Teleki
K3	DayGlo® A-14N Pigment (Fire Orange)	Wacker Vinnol H 15/45 M Vinyl Copolymer Thermoplastic	Plastic	Modified Formulation #5 and #7, Yasso (1966) and Teleki (1966)

In summary of this laboratory phase, Formulation K1(paint/varnish type) was very prone to clumping, the drying time was greater than 1 h, and both the acrylic lacquer and toluene required to thin the lacquer were expensive. Formulation K2 (resin type) also was prone to clumping, had an extended drying time, and required extra ventilation and handling measures due to the chemistry of the binding agent. Formulation K3 (plastic type) was initially made with Methyl Ethyl Ketone (MEK) and toluene following Yasso (1966). After consulting the literature on the selected thermoplastic, acetone was substituted for the toluene in a subsequent batch. Yasso Formulation #7 was modified with the use of a solution of raw pigment and solvent rather than acrylic lacquer, similar to Yasso Formulation #5. A vinyl chloride/vinyl acetate copolymer (Teleki 1966) was used in place of a carboxyl-modified vinyl copolymer. Formulation K3 coated evenly, did not clump and dried to the touch in less than 10 min during laboratory testing.

The use of multiple colors is useful for the concurrent tracking of sediments from different temporal or spatial tracer injections. DayGlo® Color Corp., a pigment company, offers a line of products that includes a total of 10 A and AX fluorescent pigment colors and 13 different D fluorescent dye colors. During the laboratory testing phase, tracer batches were produced using a coating of Formulation K3 in six fluorescent colors (table 2). These tracers were examined under UV light prior to large-scale production.

Table 2. Six fluorescent pigment colors tested in coating formulation (USGS photograph).

DayGlo® name	DayGlo® ID	Visible color	Ultraviolet color
Fire Orange[1,2]	A-14N	Orange	Orange →
Arc Yellow[1]	AX-16-N	Dark Yellow	Yellow
Signal Green	AX-18-N	Green	Yellow-Green
Horizon Blue	A-19	Blue	Blue
Carona Magenta	A-21	Pink	Orange-Pink
Columbia Blue[1]	D-298	Not Visible	Blue

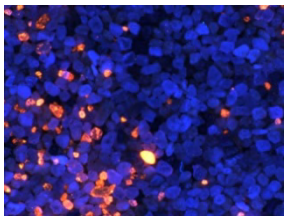

[1]Produced as a tracer for use at the Holiday Beach study site. [2]Shown under UV light in the embedded image.

Observations under UV light revealed a similarity in some fluorescent colors that could inhibit the differentiation of tracers, particularly with automated image analysis techniques. An additional feature of UV-based tracer detection is that it makes possible the use of pigments that cannot be seen in the visible spectrum. This presents opportunities for the use of tracer grains in field experiments on more populated beaches without causing a visual disturbance or inviting human tampering.

Production

Tracer production was conducted at the U.S. Geological Survey (USGS) Marine Facility in Santa Cruz, California, during May-June 2010. Initial laboratory test batches of 1,000 cm^3 were scaled up to 2–3 ft^3 batches and a total of 1.3 m^3 of fluorescent sand was created over a period of 4 non-consecutive days by two workers. Coating was performed using a 3.5 ft^3 capacity cement mixer to ensure uniform coverage and a fast drying time (Silva and others, 2007). Larger batches could be produced on a shorter timescale with the use of a high capacity cement mixer as long as the time within the mixer is increased to allow for adequate drying. Weather conditions during this process consisted of low winds, temperatures of approximately 70±10°F, and approximately 75±15 percent humidity.

The method for preparation and application of the coating is illustrated in figure 3:

1. Combine 2 L of acetone with 800 mL of pigment/dye powder to create the pigment mixture.
2. Very gradually combine 200 mL of Vinnol H 14/45 M powder into a 1 L acetone/1 L MEK mixture until fully dissolved, to create the binding agent. Stir continuously to avoid clumping.
3. Add pigment mixture to binding agent and blend to a colloidal state.
4. Pour fluorescent tagging formulation over about 2.5 ft^3 (0.071 m^3) of dry sand in a rotating cement mixer. Allow to coat and dry in rotating mixer for 10–15 min.
5. Pour tracer sand onto a tarp and air dry while manually breaking apart any remaining clumps with a rake or shovel.

Experimentation involving slight variations to the proportions of components in the described preparation is recommended to attain a coating appropriate for the mineral composition, angularity, and grain-size distribution of the native sand. For example, inadequate fluorescence per grain can be rectified by the addition of more pigment powder in step 1. The quantities presented above created the highest quality fluorescent tracer out of the sand from Holiday Beach.

Figure 3. Illustration of the production steps involved in making coated fluorescent tracers (USGS photographs).

Adverse environmental factors, such as hot weather and high humidity, led to a noticeable increase in the amount of clumping during the drying process. This clumping could be reduced by the addition of extra acetone or by extending the amount of drying time in the cement mixer to 30 minutes. Additionally, the formation of “gooey” aggregates and uneven coating occurred when too much MEK was used in proportion to the resin powder. This variation in pigment behavior between different colors was observed during the production process. This was most likely a result of changing environmental factors or the suspension of pigments in resin mixtures that did not contain an ideal ratio of liquid components during batch experimentation.

There are several obstacles associated with the presented tracer preparation. The use of chemicals such as acetone and MEK requires adequate storage facilities, safe handling, and use of protective gear during the formula mixing process. Masks with organic vapor filters are necessary for protection from the chemical fumes as well as fine particulate components, such as the pigment powders and resin. In some locations, the release of large quantities of organic vapors associated with this tracer preparation will require the acquisition of an environmental permit from the local air-quality regulating body. These factors may inhibit the on-site production of this type of tracer on many beaches in the United Status.

Tracer Evaluation

The performance of the tracer grains and the merits of the selected formulation were evaluated in the laboratory and during the course of the field experiment on Holiday Beach. The tracers were tested for seawater insolubility, abrasion resistance, and fade resistance. The toxicity and price of the tracer also are presented. A comparison of the original native sand to the tracers provides a summary of the hydrodynamic differences and limitations to the coating method of tracer production.

In regard to seawater insolubility, the technical literature for Vinnol H 15/45 M recommends using this polymer over other polymers for marine applications, stating that films of Vinnol H 15/45 M are highly resistant to water. This agrees with the findings of Teleki's (1966) review of tracer binding agents, which describes vinyl chloride/vinyl acetate copolymer thermoplastics as not affected by saltwater, alkalies, or non-oxidizing acids. Teleki (1966) also reported that this type of binding agent does not react with soluble salts in beach sand, retains fluorescence well, is ideally suited for quartz rich beaches, and has excellent resistance to the absorption of sea water, even under prolonged submersion.

The technical literature for Vinnol H 15/45 M also highlights the polymer's excellent adhesion to mineral substrates and high film strength, two important elements to resisting abrasion in the surf zone. To test this resistance in the laboratory, a sample of the Fire Orange tracer grains was placed into a hexagonal rock tumbler with salt water and abraded for approximately 1 month. Samples of the tumbled tracer material were pulled out at regular intervals (fig. 4) and visible fluorescent material was still present on most of the grains at the end of this test.

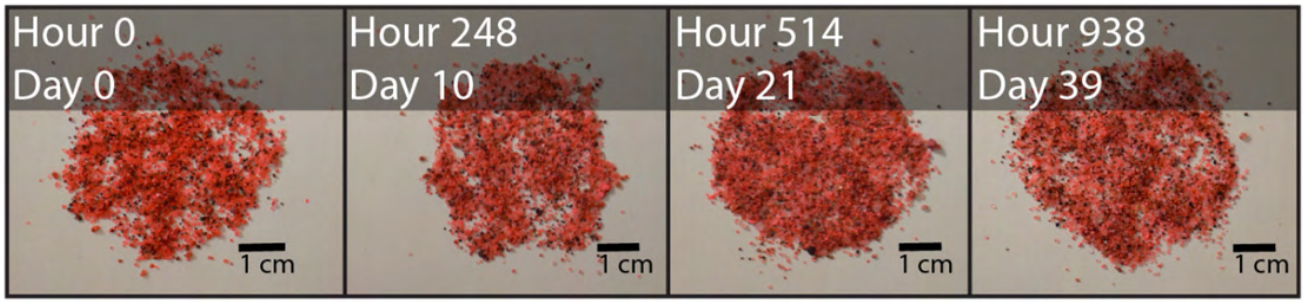

Figure 4. Photographs of tracer material that has undergone abrasion testing for up to 39 days (USGS photographs).

A direct test of fade resistance or loss of UV fluorescence was not conducted; however, the technical literature for the DayGlo® A/AX pigments cites an outdoor fluorescent lifespan of more than 3–6 months depending on the pigment (AX pigments have a longer lifespan in direct sunlight than A pigments). The partial solubility of these thermoplastic pigments in acetone, a primary component used in the coating process, may reduce the fluorescent lifespan. The effects of partial solubility are expected to be minimal based on communications with the DayGlo® laboratory. DayGlo® D pigments are organic dyes not housed in thermoplastics; they are expected to have shorter fade times but are available in a wider range of colors. Based on the dye class of D-298 (Columbia Blue), the fade time for the D pigments is around 500 h. The use of vinyl thermoplastic as a binding agent helps to maximize the light-fastness of the selected dyes and pigments, and the expected fluorescent fade times are acceptable for any planned study duration of less than 1 month.

The pigments and dyes in the described formulation are contained in the binding agent once properly dried. The Vinnol H 15/45 M Material Safety Data Sheet reports "no expected damaging effects to aquatic organisms." The MEK and acetone used in the production process are evaporated

before introduction to the marine environment. To remove any traces of MEK or acetone impurities left on the coated sand, the tracer may be rinsed prior to release at the study site.

Of the tracer formulas that were tested and considered, Formulation K3 was the least expensive option. Cost was reduced with the substitution of acetone for toluene (this also decreased odor and drying time). The direct use of pigments is recommended over the use of acrylic lacquers because price, odor, and clumping of tracer grains are all reduced. The average price for the required production materials in 2010 U.S. dollars is approximately $650.00/m^3, with variations due to choice of fluorescent color.

Tracers composed of coated native sediments repeatedly have been found to have hydraulic properties similar to those of the original uncoated particles (Ingle, 1966; Madsen, 1987). This is especially true for very thin coatings; the strength of the binding agent in the presented formulation allows the coating to be very thin and still resist abrasion. Yasso (1966) reported that vinyl thermoplastic formulations resulted in coatings of less than 0.013 mm. The quartz-rich sand used in the experiment at Holiday Beach was sieved before and after the coating process (fig. 2). The apparent coarsening trend in the grain-size distribution of the tracer relative to the sand in the original source pile can be partially attributed to the coating thickness but is more likely a result of the loss of fines, or winnowing of the tracer sand during production and transport.

A theoretical calculation of the rate at which tracer density varies with grain size under different coating thicknesses (fig. 5) predicted that the density of the tracers in this experiment (median diameter of 0.33 mm) would be an average 0.29g/cm^3 less than the native sand. The measured variation in density (fig. 5) was slightly less (approximately 0.20 g/cm^3) than the estimated amount. This may be explained by a presence of heavier mafic minerals in the sand composition, the winnowing and loss of the fines or tracer coatings that were thinner than predicted.

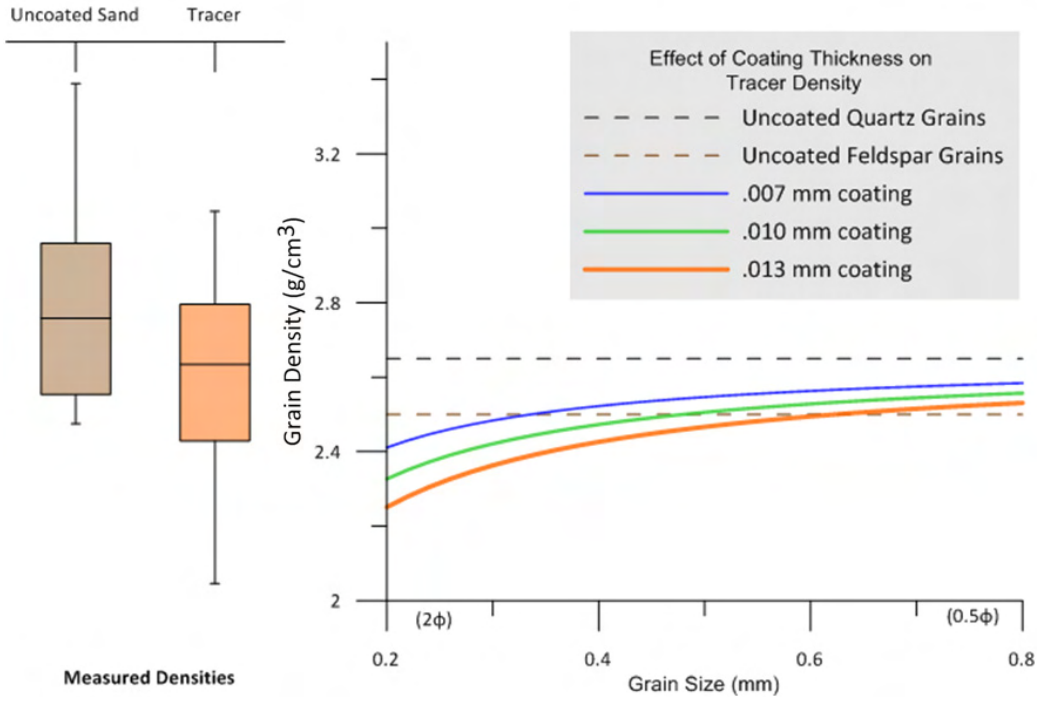

Figure 5. Graph showing a theoretical calculation of the effect of coatings of various thicknesses is shown in the plots to the right with the densities of quartz and feldspar shown for reference. The result of repeated measures of the density of the sand and tracer used in this experiment is shown to the left.

Field Experiment

Setting and Conditions

The experiment site is a beach located at the eastern end of the Santa Barbara Channel in southern California (fig. 1). The area lies within the Santa Barbara littoral cell which has a net longshore drift rate of approximately 803,000 m^3/yr to the east/southeast (Patsch and Griggs, 2008). Just downcoast of the experiment site, Mugu submarine canyon extends almost to the beach near the entrance of Mugu Lagoon and is the presumed terminus or primary sand trap of the Santa Barbara littoral cell.

Surface currents in the region near the study area are bidirectional along the coast, with mean current speeds generally less than 10 cm/s (Harms and Winant, 1998). Meteorological data from two National Oceanic and Atmospheric Administration buoys located just offshore from the study area indicate that dominant winds are from the west/northwest. The wave regime in the area also is characterized by westerly/northwesterly seas with occasional long-period, southerly swells (Xu and Noble, 2009). Over the course of the tracer experiment (September 7–11, 2010) weak, southerly swells typical of the summer wave climate were interrupted by two pulses of strong westerly sea events (fig. 6).

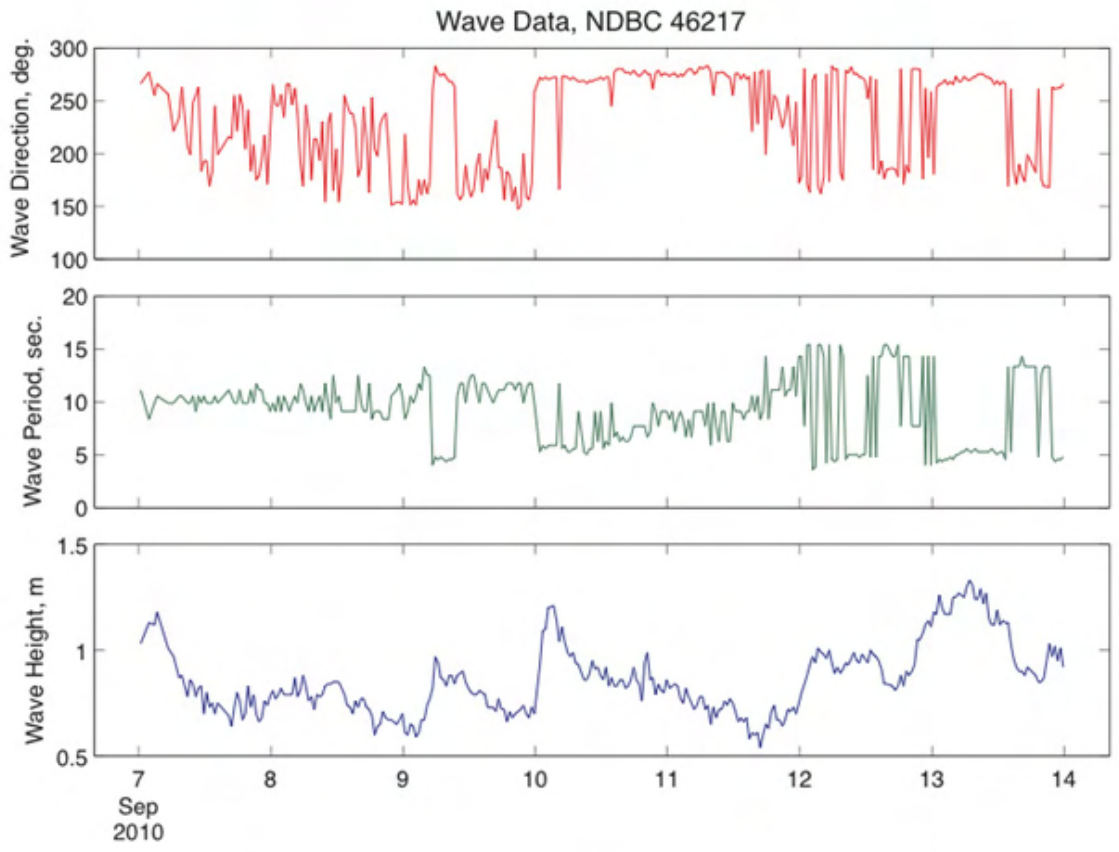

Figure 6. Graphs showing wave climate during and after the experiment, derived from the nearest National Data Buoy Center buoy, located in 110 meters of water, 30 kilometers to the west-northwest from the tracer release site.

The region experiences mixed semi-diurnal tides with a mean diurnal range of approximately 1.7 m. The tracer experiment was conducted during spring tides with a semidiurnal range of 1.3–2.1 m. The width of the study area beach from the low water line to upper berm is approximately 30–40 m including an intertidal shoreface of 8–13 m wide.

Each year, the beaches in the study area undergo a geomorphic winter-summer cycle. This pattern is most dominantly characterized by the development of a flatter berm as a result of accretion in the lower-energy summer months, which effectively increases the beach slope in front of the berm. In the winter, most of the summer berms are eroded by high energy waves, effectively reducing the overall beach slope in the foreshore.

Table 3 provides a temporal and spatial overview of grain size parameters for the coastal sediments from throughout this study. The study area is composed of medium sand beaches that are moderately well-sorted with fine to very fine sand (decreasing in diameter with depth) in the offshore. Mean grain size on the shoreface increased from east to west as the beach narrows around an exposed, armored bend in the coastline (figs.1 and 7) and decreases again on the more sheltered beach near the head of Mugu Canyon. In April and September, mean grain size increased with distance from the swash zone to the berm. At the berm top, the observed decrease in grain size is most likely due to aeolian deposition. Temporal changes in the grain-size parameters at the release site are characterized by an approximately 90 μm decrease in the mean diameter over a 5 month period, likely a result of accretion in a lower energy summer wave climate.

Table 3. A summary of the measured grain size parameters from samples collected throughout the study area. Locations of samples are shown in figure 1. The shoulder transect is located about 150 meters upcoast from the release site.

Sampling date		No.	Location	D_{50}	Grain size	Sorting
Regional grain sizes	April 2010	A1	Upper Beach Armored Segment	1.2 ϕ	Medium sand	Well sorted
		A2	Upper Beach Firing Range	1.3 ϕ	Medium sand	Moderately well sorted
		A3	Storm Overwash Release Site Road	1.5 ϕ	Medium sand	Moderately well sorted
	September 2010	O1	Offshore 10 ft depth	2.9 ϕ	Fine sand	Moderately sorted
		O2	Offshore 20 ft depth	2.9 ϕ	Fine sand	Moderately sorted
		O3	Offshore 35 ft depth	3.3 ϕ	Very fine sand	Moderately well sorted
		O4	Offshore 50 ft depth	3.8 ϕ	Very fine sand	Well sorted
Tracer	April 2010	-	Undyed Source Sand	1.5 ϕ	Medium sand	Moderately well sorted
		-	Dyed Tracer Sand	1.3 ϕ	Medium sand	Moderately well sorted
Release site grain sizes		A4	Upper Beach Release Site	1.4 ϕ	Medium sand	Moderately well sorted
		A5	Swash Zone Release Site	1.7 ϕ	Medium sand	Moderately well sorted
	September 2010	-	Berm Top Shoulder Transect	1.9 ϕ	Medium sand	Moderately well sorted
		-	Upper Beach Shoulder Transect	1.6 ϕ	Medium sand	Moderately sorted
		-	Lower Beach Shoulder Transect	1.9 ϕ	Medium sand	Moderately well sorted
		-	Swash Zone Shoulder Transect	2.0 ϕ	Medium sand	Moderately sorted

Figure 7. Photograph of narrow, armored segment of coastline that lies to the east of the tracer release site (USGS photograph).

Tracer Deployment and Monitoring

At low tide on September 7, 2011, tracer sediments were placed into shallow ditches across the shoreface at the Holiday Beach tracer release site (fig. 8). A volume of 0.2 m^3 Columbia Blue tracer was injected near the swash zone and 0.05 m^3 of Arc Yellow tracer was deployed just beneath the berm. The bulk of the tracer sediments, 0.34 m^3 colored Fire Orange, were placed in a 1 m wide, 0.1 m deep trough on the mid-shoreface.

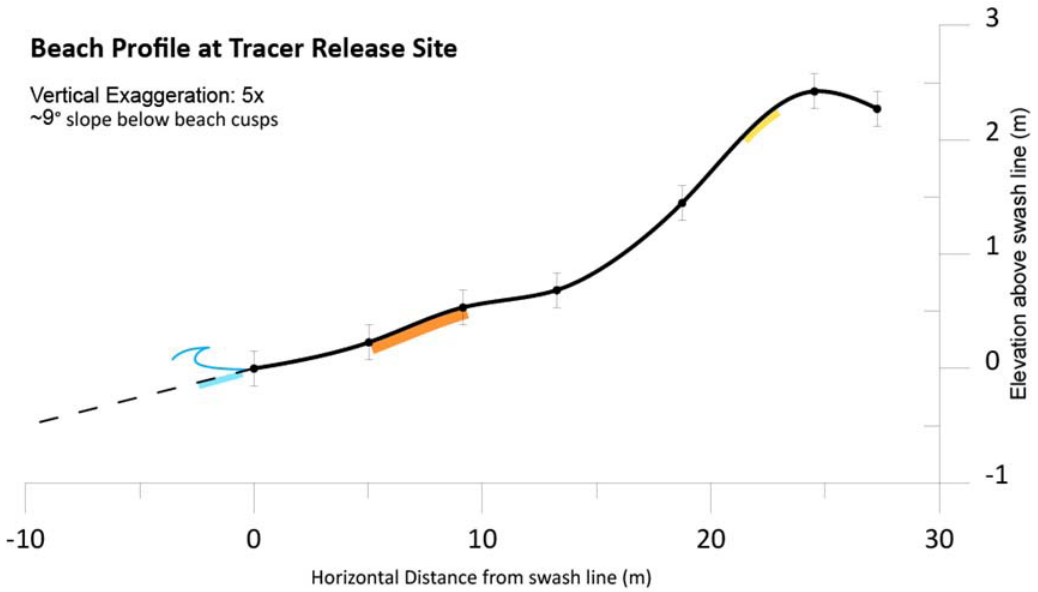

Figure 8. Graph showing profile of the tracer release site with locations of tracer injection shown.

The intended method of tracer monitoring for this experiment was an innovative two-camera setup that utilizes rapid on-site digital image analysis (algorithm for UV grain counts modified after Rubin, 2004) to capture a three-dimensional view of the tracer distribution at a grid of sampled locations on the shoreface. The general setup of the instrumentation is similar to the all-terrain vehicle (ATV)-mounted SADAM system used by Pinto and others (1994) for automated surface grain counts. In this experiment the surface camera (fig. 9*C*) was a miniature USGS eyeball imaging system (Chezar, 2001) with a UV LED light source modification. An additional vertical profiling camera (fig. 9*B*, after REMOTS, Rhoads and Germano, 1982) collected automated grain counts to a depth of 10 cm in tandem with the surface counts. The primary advantages of this system are that it is fast and that it samples the distribution of tracers throughout the mixing layer as opposed to just on the surface. The importance of sampling beyond the surface in tracer studies in order to capture a three-dimensional measure of of sediment movement is now widely recognized (Kraus and others 1982; Caviola and others 1997a).

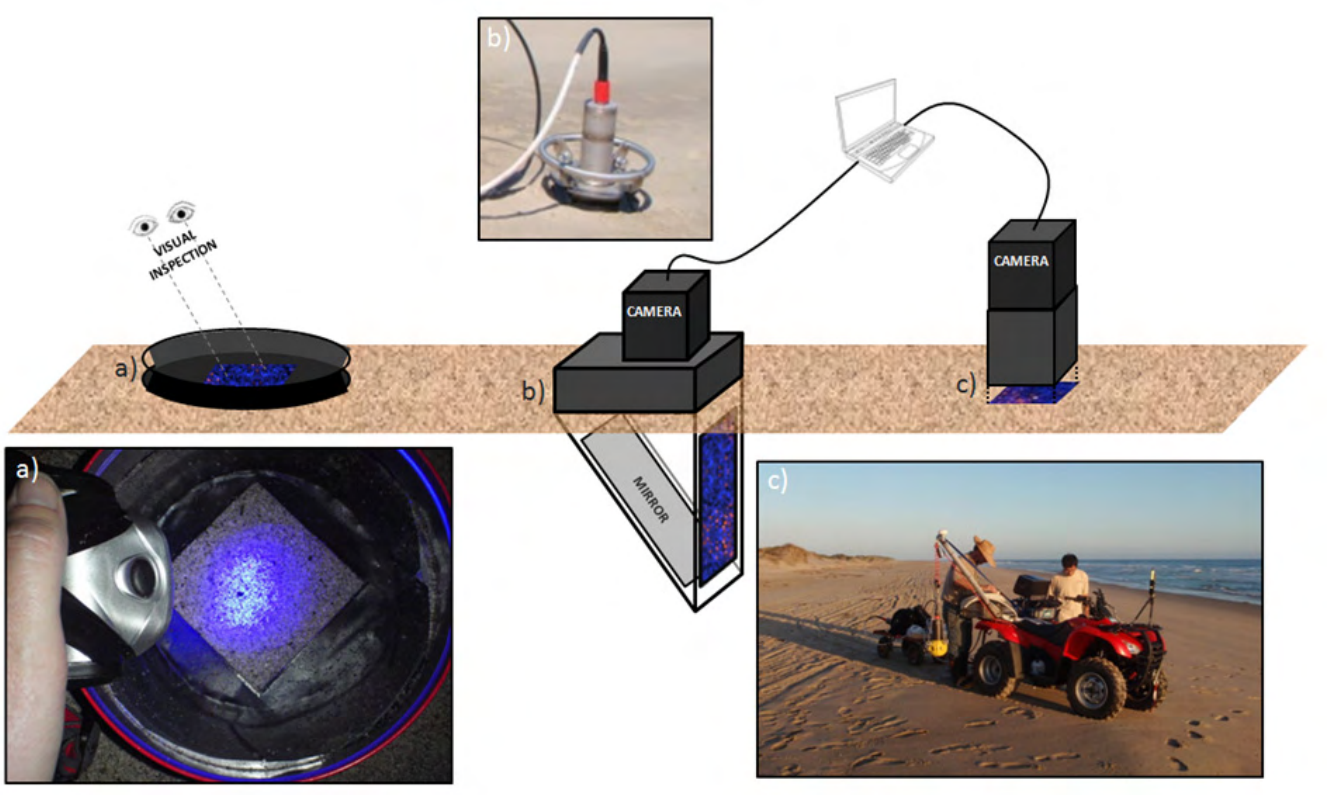

Figure 9. Graphic representation of the sampling techniques used in this experiment. Manual visual inspection (a) and push cores (not shown) were used to produce the presented results in this study. Automated image analysis using a GPS-linked vertical depth profile camera (b) and surface camera (c) mounted on an ATV platform produces improved speed and an increased sampling density.

Following the deployment of the tracer sediments, the release site was revisited for sampling at the next lower low tide, approximately 12 h later. Initial use of the ATV-mounted automated dual-camera system resulted in low grain counts of less than 1 tracer grain per image with the surface camera. A manual examination of the shoreface with UV light indicated that low returns were not a result of an absence of tracer material, but that the field of view on the camera was not adequately sized to capture useful automated grain counts following initial dispersal of the material. Because of these low

returns, a method of grain counts based on visual inspection (fig. 9*A*) with a hand-held UV light sources was adopted.

Manual surface grain counts were conducted on a grid of cross-beach transects every 20 m along the shoreline in each direction away from the profile where tracer injection occurred (fig. 10). On average, there were at least four grid points on each cross-beach transit. At each grid point a visual count of tracer grains within a 3×3 in. area was conducted in triplicate and the average of these three counts was recorded. The geographic position of each observed grid point was recorded with a handheld Global Positioning System (GPS) receiver.

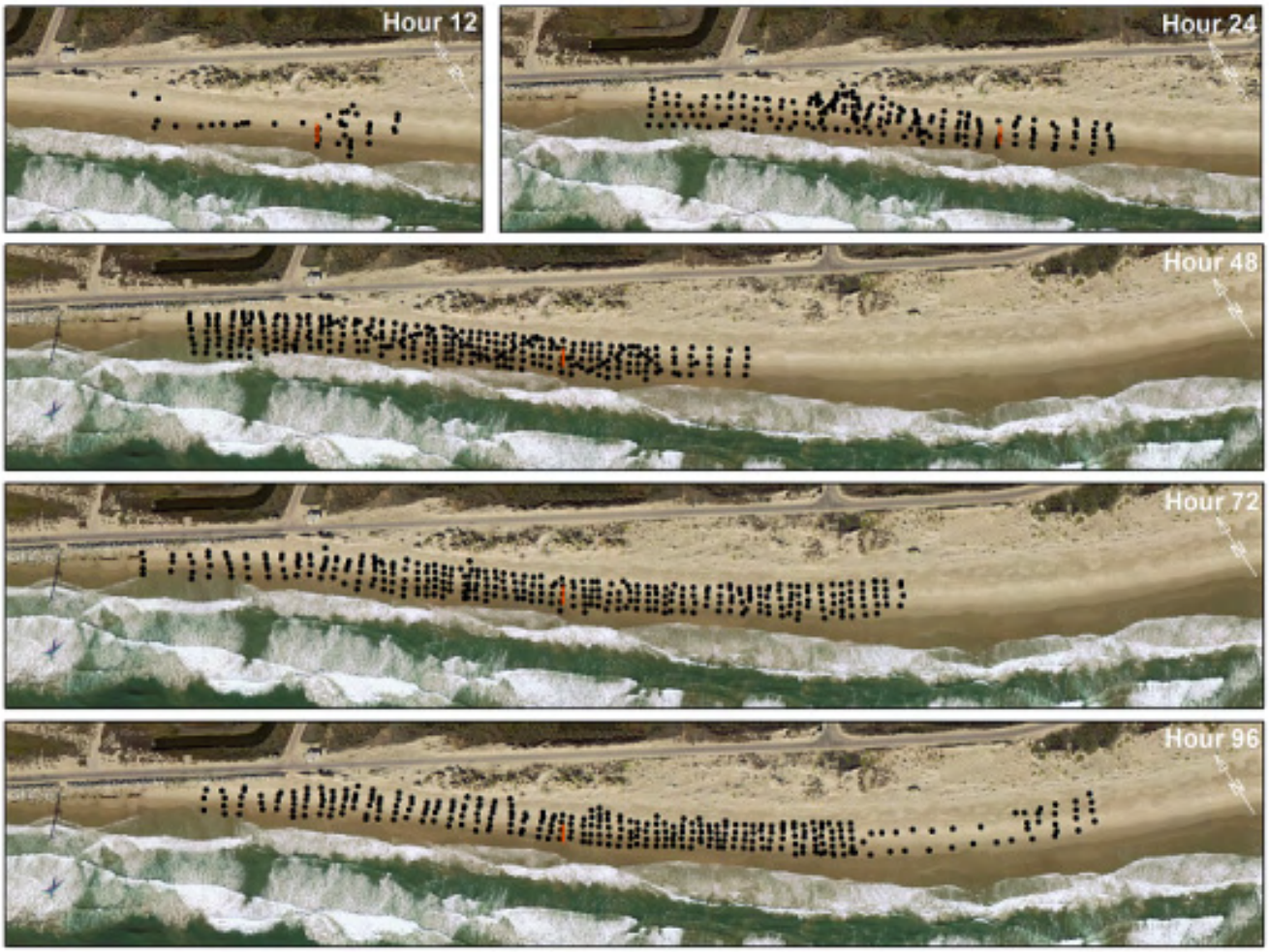

Figure 10. Aerial photographs of the study area displaying the distribution of the tracer grain count measurements from hour 12 to hour 84 (USGS orthorecified aerial photograph, October 1, 2004). The tracer injection site is highlighted in orange.

Surface distribution of tracer grains was observed at successive low tides (an approximately 12-h interval) using the visual inspection technique for a total duration of 84 h (h12 – h84). Because of military training operations in the restricted use-area surrounding Holiday Beach, interrupted surveys (h12) and restricted access combined with unfavorable light conditions (h48 and h72) resulted in some gaps in observation.

A very limited number of Arc Yellow and Columbia Blue tracers were identified by visual inspection during the h12 observation. The low number non-Flame Orange tracer observations may be attributed to a combination of three factors: (1) a sufficient volume of these tracer colors was not deployed, (2) a significant portion of the tracer material deployed in the swash zone was carried offshore by wave action, and/or (3) these colors, while tested with the automated camera system, are less visible to the naked eye under UV light. As a result of the low recovery rate for these tracer colors, only Flame Orange tracer counts were made at successive observation times and an observed distribution of these tracers has been included in the remainder of this report.

In addition to the surface counts, push core samples were taken 24 h after the tracer release along three cross-beach transects near the release site. The transects were located at the cusp (five samples), at the horn (eight samples), and at the shoulder (seven samples) of the same berm feature, as shown in figure 11. Each push core was vertically sub-sampled into 1-cm sections in the laboratory and the number of tracer grains in each section was visually counted. Four push core samples from the shoulder transect were sieved in the laboratory and a visual count of tracer sediments within the grain-size distribution was conducted (method after Komar, 1977).

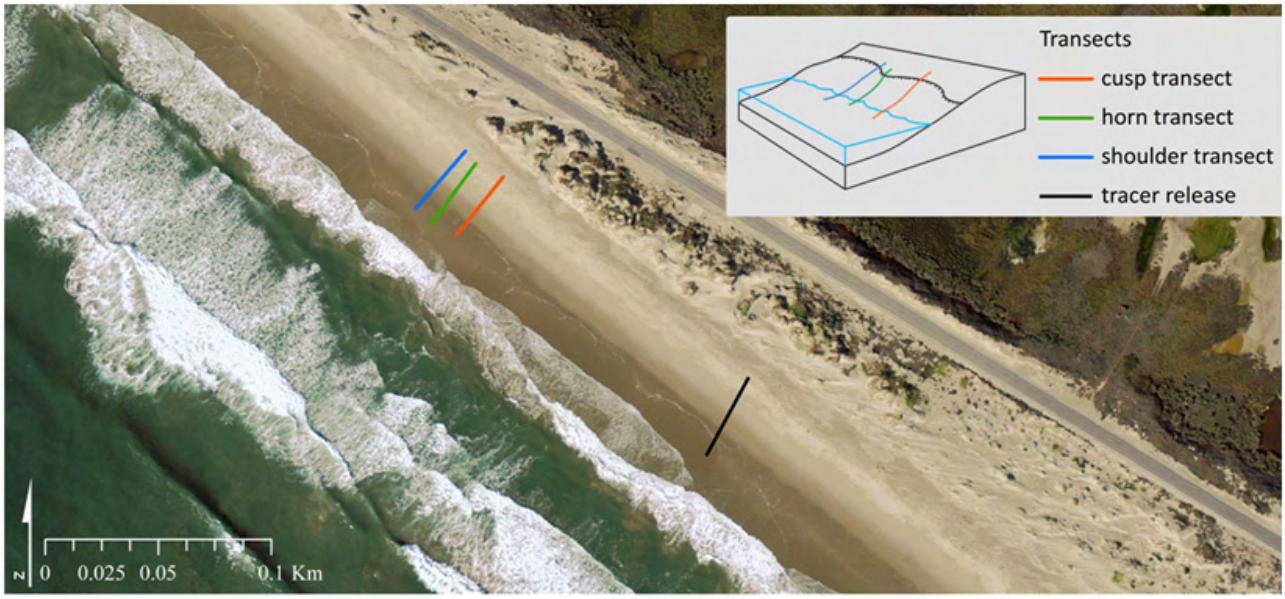

Figure 11. Aerial photograph with location of push core transects relative to the tracer release profile and the rhythmic beach cusp morphology of the berm (USGS orthorecified aerial photograph, October 1, 2004).

Results and Discussion

The field surveys of surface tracer counts, illustrated in figures 10 and 12, exhibit a complex dispersal pattern that appears to include both advection and diffusion processes. The number of tracers observed near the initial release site decreased rapidly with time. Concurrently, the total area of the shoreface where tracers were observed expanded with time as the tracer grains were dispersed by wave action; the length of beach where tracers were observed increased from 500 m at h24 to more than 1,000 m at h84 contributing to a decrease in the net tracer density.

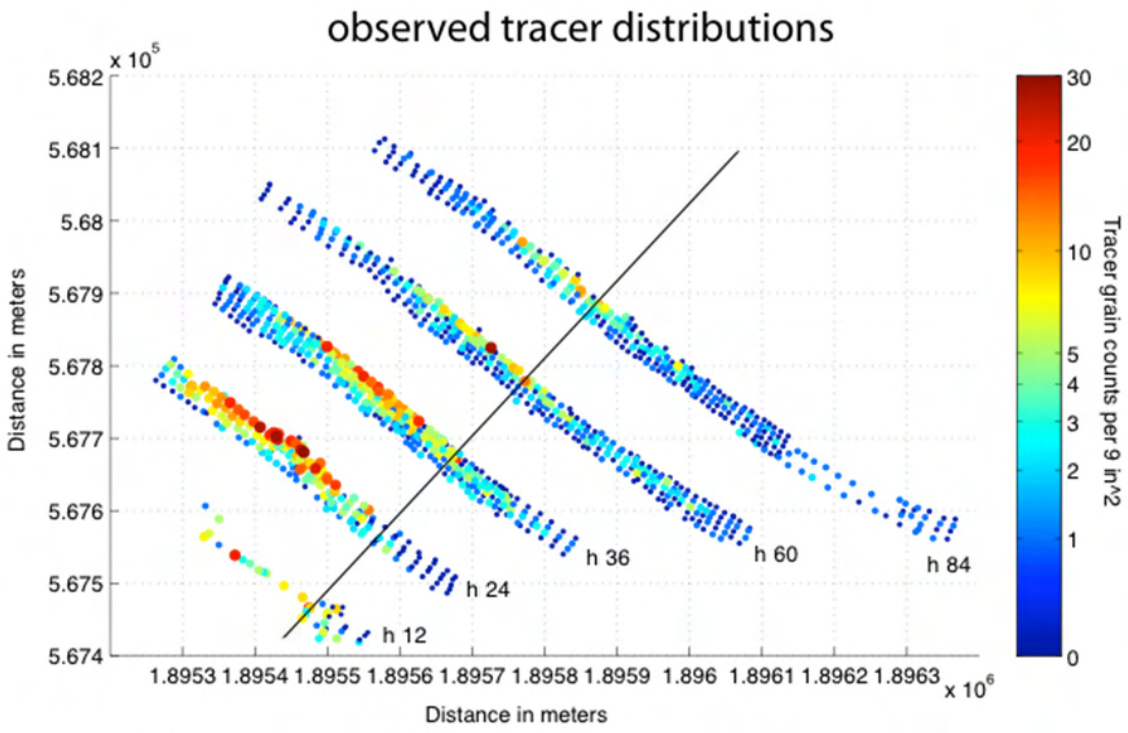

Figure 12. Scatter plot of the spatial distribution of tracer counts from five sequential surveys, each conducted at low tides, after the tracers were released at h0 (about 3:30 p.m., September 8, 2010). The number of tracer grains at each survey point is displayed (on logarithmic scale) by both the color and the size of the plotted points. For clarity, the coordinates of the scatter plot are shifted 100 meters diagonally for each survey.

In this experiment, a spatial integration method was used to analyze tracer advection (Madsen, 1987). To quantify alongshore transport of the tracer material, centroids were computed using the center-of-mass concept (Silva and others, 2007) for each individual survey. The centroid positions did not exhibit a unidirectional movement of the tracer material. Twelve hours (h12) after the tracer release, the centroid moved about 50 m upcoast. At h24 the centroid moved 150 m farther upcoast, with an average velocity of transport of 20 cm/min (figure 12).

From h36 through the remainder of the experiment observations, the centroid movement reversed to a downcoast direction. At h36, h60, and h84, the centroid migrated in the downcoast direction 50, 100, and 50 m, respectively. Thus, the centroid was located near the initial release site at h84 after a downcoast transport with an average velocity of 6 cm/min.

The upcoast migration and subsequent reversal of the centroid can be readily explained by the strong westerly wave events illustrated in figure 6. Because the region is more typically characterized by a summer wave climate similar to the conditions in the latter half of the experiment, the slower, downcoast movement of the centroid may be used as a representation of the typical alongshore sediment advection at this location.

The results of the across-shore vertical sampling are summarized in figure 13. The presence of tracer grains throughout the push cores indicated a mixing depth (or transport thickness, Balouin and others, 2005) of at least 8 cm. This estimate is corroborated by the fact that there was no layer of tracers left at the release location—all tracers initially placed in a 10 cm deep pit were completely mixed and removed.

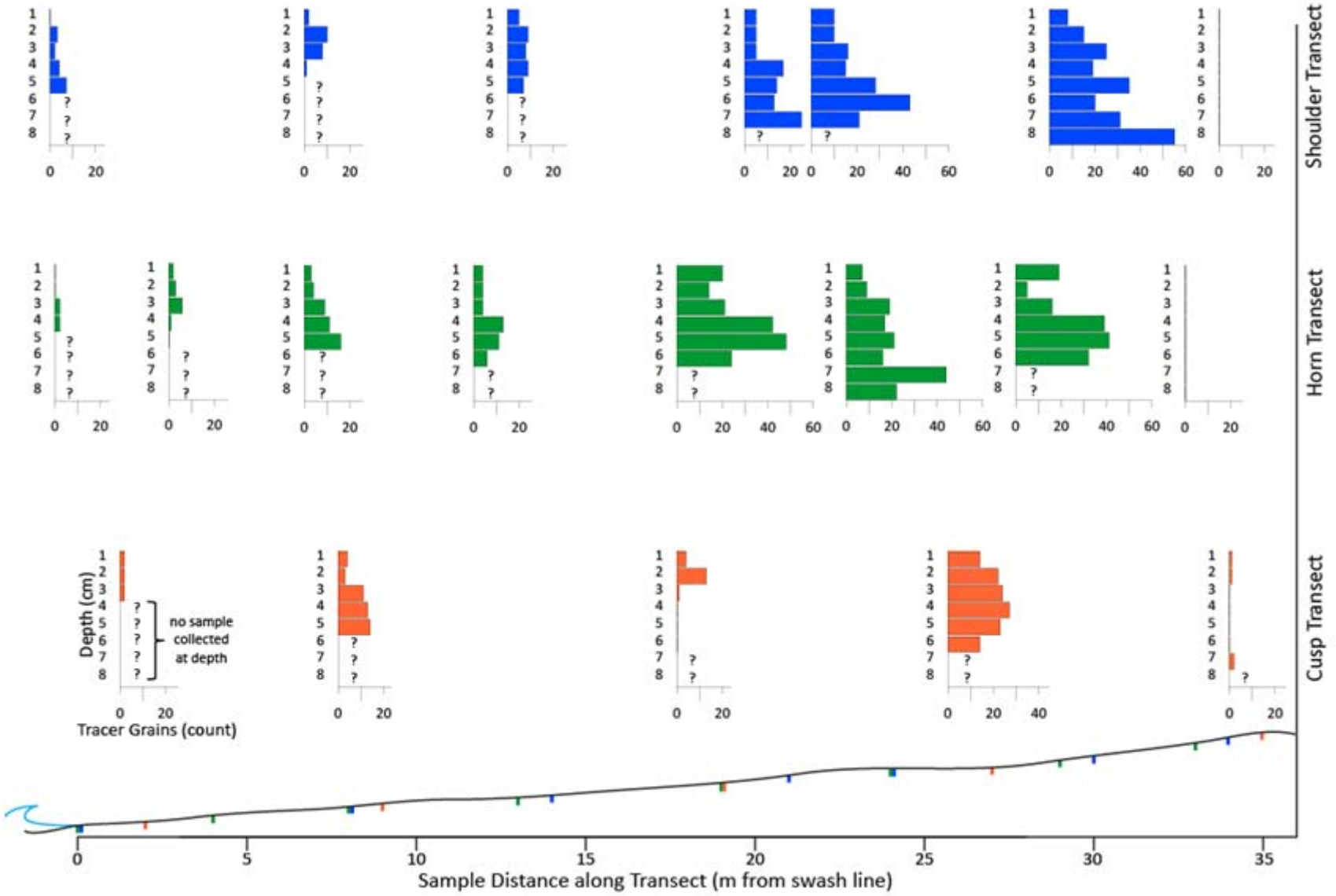

Figure 13. Histograms of vertical tracer grain counts in each push core sample arranged by transect location and distance across the shoreface. Push core samples of less than 8 cm are indicated by question marks (*?*).

Many tracer studies that rely on surface observations alone have assumed uniform distribution down to burial depth; the results of the push core grain counts in this experiment highlight the importance of using a three dimensional approach. The majority of push core samples exhibited considerable variation in the number of tracer grains with depth. Only 17 percent of the push cores that contained any tracer had a near uniform vertical distribution and, as seen in many of the histograms in figure 13, the total number of tracer grains at depth was often 2–4 times greater than the number of grains observed in the top 1 cm interval.

The across-shore distribution of tracer material suggests an initial onshore movement of the tracer as the centroid migrated upcoast, this pattern also can be observed in figure 12. One explanation for this pattern is an onshore movement of sand associated with the high energy wave event, another explanation could be that advection dominates in the upper one-half of the intertidal zone where wave surges prevail and that diffusive processes dominate on the lower one-half shoreface where breaking waves are more prevalent over a typical tidal cycle.

The differences in tracer distribution from horn to cusp allude to the role of local circulation patterns around this type of beach morphology. Uprush against the horn and shoulder is in contrast to the swift backrush flows that typically occur perpendicular to the cusp and may account for the decreased tracer deposition along the cusp transect. Furthermore, the observation of grains atop the berm only at the convergence point is further evidence of this pattern. Although this type of interpretation can only be speculative in this study, it demonstrates the potential to use tracer studies to not only calculate traditional rates of littoral drift but also to validate complex nearshore hydrodynamic circulation models.

The results of the across shore distribution of tracer sediments by grain size are presented in figure 14. At each location across the beach, the distribution of tracers by size closely follows the native sand distribution. A high ratio of coarser tracers on the upper beach, relative to lower down, in conjunction with the tracer diameters on the lower one-half of the shoreface being skewed towards fines, indicates that the tracers are undergoing the same across shore size sorting that is seen in the native beach sand. Both of these patterns are evidence that the tracer grains and the uncoated sand are behaving in a hydrodynamically similar way.

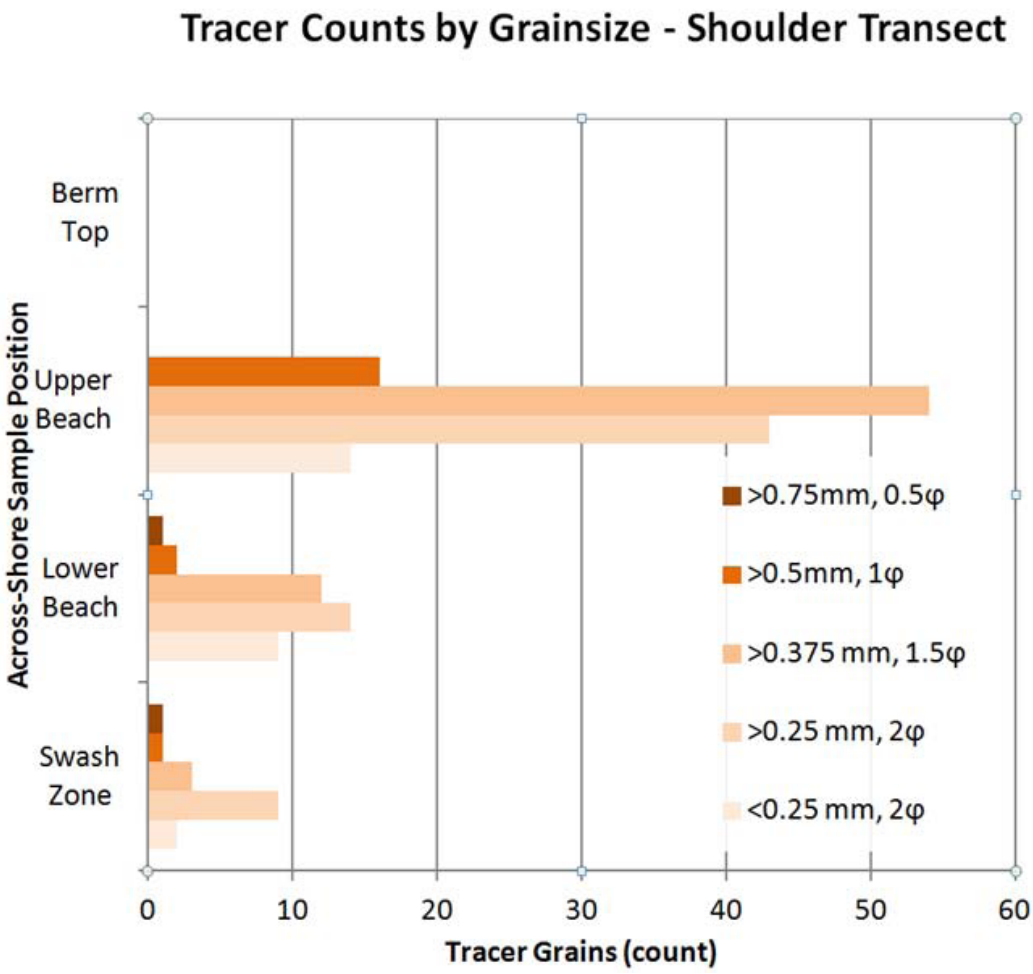

Figure 14. Histograms illustrating the across-shore distribution of tracer grains on the shoulder transect as a function of grain diameter.

Summary and Recommendations

Like other contemporary sand tracer studies, we found that minor modifications to the formulations and methods presented by Yasso (1966) resulted in a suitable fluorescent coating for the USGS tracer study at Mugu Canyon. The selected formulation for use in this study consists of sand evenly coated in a thin layer of DayGlo® thermoplastic pigments/dyes in a colloidal mixture with Wacker Vinnol H 15/45 M, a vinyl chloride/vinyl acetate copolymer thermoplastic. The measured density of the tracer grains were slightly less than the native sand, as predicted, but the tracer performance in the field indicated that the differences in the hydrodynamic properties of the tracer grains were at an acceptably low level for the tracer to mimic the behavior of the native beach sand. Based on the results of the grain-size analysis, studies that seek to use a similar methodology would be advised to collect native beach sand from the beach close to the time of tracer deployment to minimize the effects of seasonal grain-size variability. A preferred method of tracer preparation would be on-site.

The results of the field experiment demonstrated the importance of selecting an appropriately sized field of view or observation window for automated tracer grain detection methods. Manual grain counts and laboratory analysis were time consuming so further development of the automated system

would streamline experimental observations and improve recovery rates. The overall results of the tracer monitoring post-injection were quantitatively inconclusive due to the limitations of the observation methods. By assuming that the tracers were fully mixed with native sand within a 10 cm mixing depth, an estimated tracer recovery rate using the manual method (White, 1998) can be computed based on a 40 m beach width, the beach length, grain size, and a nominal sediment porosity value (0.65). This recovery rate was the highest (71 percent) at h24, and decreased to 50, 31, and 33 percent for the surveys at h36, h60, and h84, respectively. Only the h24 recovery rate fell into the "good" tracer experiment criteria (>60 percent) as defined by White (1998).

Calculations of required tracer volume should include a consideration of the camera field of view. Equation 1 is presented as a guideline to assist researchers in selecting a minimum volume of tracer (V_{tracer}) based on study site characteristics and the scale of the observation window.

$$V_{tracer} = \frac{L_b W_b d_{ML}}{\left(A_{FOV} / \left(\left(\frac{D_{50}}{2}\right)^2 \pi\right)\right) \eta R_r} \quad (1)$$

Where
L_b is length of beach over which tracers will be observed (m)
W_b is active experimental beach width (m)
d_{ML} is depth of the mixing layer (m)
D_{50} is average grain size (m)
A_{FOV} is area of the camera field of view or observation window (m^2)
η is beach porosity value (-), and
R_r is recovery rate (%)

This equation will yield an approximation of the minimum volume of tracer required for observations of more than one tracer grain/surface image. Because recovery rates decrease as a function of time, the recovery rate should be selected as a function of the duration of the field experiment.

Based on the experimental counts of tracer per observation window (58 cm^2 field of view) and using the beach characteristic assumptions from the recovery rate calculation, the average grain counts would have been less than 0.6 grain per image at all experimental time steps if the automated camera system (6 cm^2 field of view) had been used. This is consistent with the extremely low number of tracers (typically zero) observed in images that were collected with the camera system at h24. To achieve meaningful tracer observations (an average tracer grain count of more than one per image), the minimum field of view for the automated camera system would have needed to be at least 52 cm^2 for the 0.34 m^3 volume of tracer with a 30 percent recovery rate by h96. Conversely, using the volumetric beach assumptions above, we can calculate that this experiment would have required an initial tracer injection of 0.8 m^3 for the designed camera to be effective with a 100 percent recovery rate. Given the actual recovery rates, which account for sand lost to the nearshore, an initial tracer volume of 2.4 m^3 (more than 7× the amount deployed) would have been necessary to obtain useful measurements with the designed camera system.

A preliminary modeling study that investigated the movement of the tracers described in this field experiment over a 1 week period and in a range of typical nearshore wave climates concluded that the tracer material would not bypass the canyon head (Xu and others, 2011). Depending on the relative strengths of surfzone currents at the head of Mugu Canyon and in the downcoast direction, the modeled path of tracers is either onto the offshore shelf or into the canyon head. A longer term field investigation with an adjusted camera system could be used to verify these model results.

Acknowledgments

The authors would like to acknowledge Hank Chezar and Joanne Ferreira from the USGS Pacific Coastal and Marine Science Center for their significant roles in the field component of this tracer experiment as well as in the development and testing of the camera system. Steve Granade and Martin Ruane, from the Ventura County Naval base, were instrumental in facilitating the execution of the beach experiment within rules of the restricted use areas. The manuscript benefited from the insightful reviews by Lissa MacVean and Li Erikson from the USGS Pacific Coastal and Marine Science Center. This study is funded by the Coastal and Marine Geology Program of the U.S. Geological Survey.

References Cited

Balouin, Y., Howa, H., Pedreros, R., and Michel, D., 2005, Longshore sediment movements from tracers and models, Praia de Faro, South Portugal: Journal of Coastal Research, v. 21, no. 1, p. 146–156.

Black, K.S., Athey, S., Wilson, P., and Evans, D., 2007, The use of particle tracking in sediment transport studies: a review, *in* Balson, P. and Collins, M.B. eds., Coastal and shelf sediment transport, Geological Society Special Publications: Geological Society of London, London, v. 274, p. 73–91.

Boon, J.D., 1970, Quantitative analysis of beach sand movement, Virginia Beach, Virginia: Sedimentology, v. 17, p. 85–103.

Chezar, H., 2001, Underwater microscope system: U.S. Geological Survey Fact Sheet 135-01, 2 p.

Chapman, D. M., and Smith, A.W., 1977, Methodology of a large scale sand tracer experiment: Proceedings of the 3rd Australian conference on coastal and ocean engineering, p. 185–189.

Ciavola P., 2004, Tracers *in* Schwartz, M. ed., Encyclopedia of Coastal Sciences: Dordrecht, The Netherlands, Kluwer Academic Publishers, p. 1253–1258.

Ciavola, P., Taborda, R., Ferreira, Ó., and Dias, J.A., 1997, Field observations of sand-mixing depths on steep beaches: Marine Geology, v. 141, no. 1–4, p. 147–156.

Ciavola, P., Taborda, R., Ferreira, Ó., and Dias, J.A., 1997a, Field measurements of longshore sand transport and control processes on a steep meso-tidal beach in Portugal: Journal of Coastal Research, v. 13, p. 1,119–1,129.

Everts, C.H., and Eldon, C.D., 2005, Sand capture in southern California submarine canyons: Shore & Beach, v. 73, no. 1, p. 3–12.

Ferreira, Ó., Fachin, S., Coli, A.B., Taborda, R., Dias, J.A., and Lontra, G., 2002, Study of harbor infilling using sand tracer experiments: Journal of Coastal Research, special issue no. 36, p. 283–289.

Harms, S., and Winant, C.D., 1998, Characteristic patterns of the circulation in the Santa Barbara Channel: Journal of Geophysical Research, v. 103, p. 3,041–3,065.

Heathershaw, A.D., and Carr, A.P., 1977, Measurements of sediment transport rates using radioactive tracers: Proceedings of Coastal Sediments ’77, American Society of Civil Engineers, p. 399–416.

Ingle, J.C., 1966, The movement of beach sand, an analysis using fluorescent grains: Developments in Sedimentology, v. 5.

Jolliffe, I.P., 1963, A study of sand movements on the Lowestoft sandbank using fluorescent tracers: The Geographical Journal, v. 129, no. 4, p. 480–493.

Komar, P. D., 1977, Selective longshore transport rates of different grain-size fractions within a beach: Journal of Sedimentary Petrology, v. 47, p. 1,444–1,453.

Kraus, N.C., Isobe, M., Igarashi, H., Sasaki, T.O., and Horikawa, K., 1982, Field experiments on longshore sand transport in the surf zone: Proceedings of the 18th Coastal Engineering Conference, American Society of Civil Engineers, p. 970–988.

Madsen, O.S., 1987, Use of tracers in sediment transport studies: Proceedings of Coastal Sediments, American Society of Civil Engineers, p. 424–435.

Moffatt and Nichol, 2008, Regional sediment management – offshore canyon sand capture: Final Position Paper Report, 76 p.

Schwartz, M.L., 1966, Fluorescent tracer, transport in distance and depth in beach sands: Science, v. 151, no. 3711, p. 701–702.

Patsch, K., and Griggs, G.B., 2006, Littoral cells, sand budgets, and beaches, understanding California's shoreline: California Coastal Sediment Management Workgroup Report, University of California, Santa Cruz, 39 p.

Patsch, K. B. and Griggs, G.B., 2008, A sand budget for the Santa Barbara littoral cell, California: Marine Geology, v. 252, no. 1–2, p. 50–61.

Teleki, P.G., 1966, Fluorescent sand tracers: Journal of Sedimentary Research, v. 36, no. 2, p. 468–485.

Pinto, J.R.C., Dias, J.M. A., Fernandes, S.P., Ferreira, Ó., Silva, A.V., and Taborda, R., 1994, Automatic system for tagged sand detection: Gaia, v. 8, p. 161–164.

Rhoads, D.C. and Germano J.D., 1982, Characterization of organism-sediment relations using sediment profile imaging, an efficient method of Remote Ecological Monitoring of the Seafloor (REMOTS System): Marine Ecology Progress Series, v. 8, p. 115–128.

Rubin, D.M., 2004, A simple autocorrelation algorithm for determining grain size from digital images of sediment: Journal of Sedimentary Research, v. 74, p. 160–165.

Yasso, W. E., 1966, Formulation and use of fluorescent tracer coatings in sediment transport studies: Sedimentology, v. 6, no. 4, p. 287–301.

Silva, A., Taborda, R., Rodrigues, A., Duarte, J., and Cascalho, J., 2007, Longshore drift estimation using fluorescent tracers, new insights from an experiment at Comporta Beach, Portugal: Marine Geology, v. 240, p. 137–150.

White, T.E., 1998, Status of measurement techniques for coastal sediment transport: Coastal Engineering, v. 35, p. 17–45.

Xu, J.P., and Noble, M.A., 2009, Variability of the Southern California wave climate and implications for sediment transport, *in* Lee, H.J., and Normark, W. R. (eds.), Earth Science in the Urban Ocean: The Southern California Continental Borderland, Geological Society of America Special Paper no. 454, p. 171–191.

Xu, J. P., Elias, Edwin, and Kinsman, Nicole, 2011, Does littoral sand bypass the head of Mugu submarine canyon? – a modeling study: Proceedings of Coastal Sediments 2011, v. 3, p. 2,075–2,087.

Zenkovich, V.P., and Boldyrev, V.L., 1965, Alongshore sediment streams and methods of their study, *in* Proceedings of the 11th Congress of the International Association for Hydraulic Research, v. 5: Leningrad, USSR, International Association for Hydraulic Research, p. 139–148.